PHYSICAL REVIEW B VOLUME 10, NUMBER 12 15 DECEMBER 1974

Structural interpretation of the infrared and Raman spectra of glasses in the alloy system $Ge_{1-x}S_x$

G. Lucovsky, F. L. Galeener, R. C. Keezer, R. H. Geils, and H. A. Six
Xerox Palo Alto Research Center, Palo Alto, California 94304

(Received 20 May 1974)

We report a study of the infrared and Raman spectra of bulk glasses in the binary alloy system $Ge_{1-x}S_x$ ($0.90 \geq x \geq 0.55$). The spectra are interpreted in terms of models based on covalent bonding in which the $8-N$ rule is satisfied; i.e., models in which the Ge atoms are fourfold coordinated and the S atoms are twofold coördinated. For the compound composition GeS_2, $x = 0.67$, the spectra are interpreted in terms of a chemically ordered network in which the element of local order is a tetrahedral arrangement of S atoms about a central Ge atom. For the S-rich alloys, $0.90 \geq x > 0.67$, the data support a generalized chain-crossing model (CCM) rather than a random-covalent-network model (RCNM). The generalized CCM allows for a second species of S_8 rings to be in solution with a Ge-S network. The S_8 ring fraction shows a sharp increase in concentration for $x > 0.80$ indicating that on the average only one to two S atoms are incorporated between the Ge sites of the network component. For Ge-rich alloys the more limited experimental data support a restricted network model of Philipp which allows Ge-Ge and Ge-S bonds, but not S-S bonds, rather that a RCNM.

I. INTRODUCTION

There is considerable interest in the interpretation of the electronic and vibrational spectra of amorphous semiconductors in terms of chemical bonding and the resultant short-range order. Alloy systems are well suited to this type of study since the availability of a continuous variation of composition provides a convenient test of the scaling laws imposed by competing structural models. This paper reports a study of the optically active vibrational modes of the binary alloy system $Ge_{1-x}S_x$ using infrared (ir) and Raman spectroscopy. We studied bulk glasses which can be formed over a restricted, but nonetheless interesting range of compositions, $0.90 \geqslant x \geqslant 0.55$.

Our interest in this alloy system was stimulated by previous studies on the other Ge chalcogenides, $Ge_{1-x}Se_x$ and $Ge_{1-x}Te_x$. X-ray radial distribution (RDF) studies[1-3] of $Ge_{0.5}Te_{0.5}$ yield an average coordination of three, rather than six as in the crystalline phase. An average coordination of three can be achieved in two ways: by threefold coordination at each atomic site with short-range order that is related to the black phosphorous structure[4]; or by a coordination at each atomic site that satisfies the $8-N$ rule [5,6] of valence-bond chemistry (fourfold coordination at the Ge sites and twofold coordination at the Te sites). RDF studies of other alloy compositions were unable to distinguish between these models.[7] However, ir and Raman measurements on the amorphous system $Ge_{1-x}Te_x$ indicated the existence of $GeTe_4$ tetrahedra at several compositions[8] in accord with four-two coordination, ruling out the equal coordination model. There are two models maintaining four-two coordination which could be operative in the Te-rich alloy regime.[6] The first of these is a chain-crossing model (CCM) which assumes that Ge atoms incorporated into amorphous Te cross-link the twofold coordinated chains through a four-fold coordinated Ge site. This model can accommodate at most a 33% concentration of Ge atoms. The CCM implies a high degree of chemical ordering since each Ge atom is bonded only to Te atoms so that there are therefore no Ge-Ge bonds. An alternative model that can apply over the entire composition range is a random-covalent-network model (RCNM) in which the distribution of all three possible bond types, Te-Te, Te-Ge, and Ge-Ge, is based only on statistics (i.e., the composition and the covalent four-two coordination) and is not influenced by other factors such as relative bond strength. RDF studies are unable to discriminate between these two models. Spectroscopic studies using ir and Raman,[8] uv photoemission,[9,10] and x-ray photoemission[10,11] also support a local coordination that satisfies the $8-N$ rule, but also cannot distinguish between these models. RDF studies on the $Ge_{1-x}Se_x$ system[12] also support four-two coordination, but are also unable to discriminate between the two models. On the other hand, Raman studies[13] on bulk $Ge_{1-x}Se_x$ glasses support the CCM in the Se-rich regime.

We have chosen to study the $Ge_{1-x}S_x$ system using both ir reflectance and Raman spectroscopy in order to attempt a further resolution of the issue of short-range order in the Ge chalcogenides. Bulk glasses can be formed over a sufficiently wide range of compositions, $0.90 \geqslant x \geqslant 0.55$, so that the study can focus on both the chalcogenide-rich ($x > 0.67$) and Ge-rich ($x < 0.67$) alloys regimes. These two alloy regions are defined with respect to the compound composition GeS_2 ($x = 0.67$). Furthermore, the large mass difference between S and Ge makes it relatively easy to distinguish between vibrations associated with Ge-Ge, Ge-S, and S-S bonds. This is to be contrasted with the situation in the $Ge_{1-x}Se_x$ system where the almost equal masses of the Ge and Se atoms make a similar discrimination more difficult. A combination of ir and Raman spectroscopy is particularly useful in as much as the two spectra are frequently complementary in the sense that the dominant features in each spectrum occur at different frequencies. This has been demonstrated for one alloy in the $Ge_{1-x}S_x$ system, $Ge_{0.3}S_{0.7}$,[14] a composition that is very nearly equal to that of the compound. These spectra were interpreted in terms of a structural model in which the element of local order is a tetrahedral arrangement of S atoms about a central Ge atom, i.e., a GeS_4 tetrahedron. The existence of a chemically ordered structure at the compound composition is also supported by RDF studies.[15,16] The glasses that we have studied give us an opportunity to determine whether one model, for example the RCNM, is applicable for all x, or whether different models apply for different composition ranges. The existence of a chemically ordered phase at $x = 0.67$ suggests that different models could be operative in the S-rich and Ge-rich composition regimes. This is indeed supported by experiment. Our analysis of the imaginary part of the complex dielectric constant ϵ_2 as a function of alloy composition in the S-rich regime, indicates a linear behavior in the peak value of ϵ_2 with alloy composition $(1-x)$. This dependence is in accord with the CCM, but not the RCNM. For increasingly Ge-rich alloys, a very rapid loss of the sharp ir and Raman features associated with the tetrahedral grouping of four S-atoms about a central Ge-atom is consistent with a restricted random-bonding model proposed by Philipp,[17] but not with the RCNM. The more restricted model of Philipp was developed for application to the Si-O system in which the bonding considerations parallel those that also apply in the Ge-S system. As applied to the Ge-S system, the model is based on tetrahedra that are centered about Ge atoms and that have S and Ge neighbors distributed according to statistics determined only by the composition. As such the model precludes S-S bonds and is therefore more restrictive than the RCNM. Another interesting aspect of our work is the identification of S_8 rings in the S-rich alloys. This is made primarily through the Raman spectra, but is also confirmed by measurements of the ir transmittance.

The paper is organized into five sections. Section II discusses the experimental details that relate to sample preparation and characterization, and to the ir and Raman measurements. Section III presents the experimental results and indicates the methods by which the spectra were analyzed or reduced. Section IV is concerned with an interpretation of the spectra that is based on the short-range order. In that section we first consider the compound composition ($x = 0.67$) and then the S-rich and Ge-rich regimes. Section V summarizes our study. Here we also point out that the $Ge_{1-x}S_x$ system provides a bridge between two previously identified protypical classes of amorphous semiconductors, the tetrahedrally bonded amorphous solids, the group-IV elements and their alloys and the III-V's on the one hand, and the elemental and compound amorphous chalcogenides on the other. The spectra of these two classes of materials are very different from each other,[18] and our study yields some insight into the structural and topological factors that promote these differences.

II. EXPERIMENTAL

A. Sample preparation

$Ge_{1-x}S_x$ glasses were prepared by weighing high-purity germanium and sulphur into fused silica tubes. Most of the samples were prepared in 10-mm-diameter tubes and consisted of 5–10 g of reactants. The tubes were sealed off under vacuum and placed in a rocking furnace for approximately 12 h during which the temperature was increased to about (50–100) °C above the liquidus phase boundary.[19] After another 12 h in the rocking furnace, the tubes were either air quenched, water quenched, or quenched in a NaOH-H_2O solution. Our observations of the glass-forming tendency in the Ge-S system are in general agreement with previously reported results[20,21]; however, we found that the glass forming regions can be extended by quenching small quantities of the liquids into NaOH-H_2O solutions. An aqueous NaOH solution approximately doubles the quenching rates attainable for water.[22] High-S-content samples ($x > 0.8$) required air cooling from just above the liquidus to prevent frothing (presumably due to evolution of dissolved S) and Ge-rich samples required NaOH-H_2O quenching to prevent crystallization of GeS. The samples were removed easily from the tubes and no evidence of reaction with the silica was observed. Composition was verified by examining each run for additional phases; no such phases are present in any of the samples used for the ir and Raman studies. In addition, by carefully controlling heating, mixing, and cooling cycles, the reported tendencies toward phase separation in this system[20,21] were eliminated, at least on a macroscopic basis.

Specimens for optical experiments were prepared by conventional grinding and polishing techniques. Examination under cross polarizers showed inhomogeneities in the optical properties which were not evident in unpolarized light. Annealing these samples at various temperatures improved the optical properties, but did not completely eliminate the inhomogeneities. It was also observed that samples containing high sulphur concentrations ($x=0.8$–0.9) had a tendency to crystallize on surfaces that had been mechanically polished.

B. ir and Raman measurements

ir reflectance measurements were made at near normal incidence using a Perkin-Elmer Model No. 180 Spectrophotometer operated in a double-beam mode. The reflectance of the $Ge_{1-x}S_x$ glasses is normalized by comparison with the reflectance from a front surface Al mirror. The sample reflectance is measured in the range from 600 to 50 cm^{-1}; resolution is approximately 2 cm^{-1}. All measurements of the ir reflectance as well as the Raman measurements were made with the samples at room temperature.

The Raman scattering from all samples except $x=0.57$ was measured in the 90° transmission configuration, using 6250-Å radiation from a Coherent Radiation Model 490 dye laser. The $x=0.57$ sample is opaque in the range of wavelengths available, so measurements were made in the 180° backscattering arrangement, using 5145-Å radiation from a Coherent Radiation Model 52-G Ar^+ ion laser. In all cases the incident power was about 50 mW partially focussed into a spot approximately 0.5 mm in diameter. At these power densities, laser induced sample degradation was negligible during the period of time necessary to complete spectral studies on a given sample.[14] Measurements were made in both polarization cases: *HH*, where the incident and scattered electric vectors are parallel; and *HV*, where they are perpendicular. Spectral features occurred at the same wave numbers in both cases. Depolarization spectra (*HV*/*HH*) are not reported, since in several samples we found various degrees of polarization scrambling due to slight spatial variations of the effective refractive index of the material. Although these variations could not be perceived with the unaided eye, they were readily seen by inspecting the sample between crossed sheet polarizers, as in a polariscope. The existence of these inhomogeneities on a macroscopic scale does not affect the conclusions drawn in this paper from comparisons of the *HH* spectra.

III. EXPERIMENTAL RESULTS AND DATA REDUCTION

A. ir reflectance

The ir reflectance spectra of glasses in the $Ge_{1-x}S_x$ binary alloy system for values of $x=0.55$, 0.57, 0.63, 0.67, 0.75, 0.80, and 0.90 are given in Fig. 1. The spectra are displaced vertically for clarity, with the zero-reflectance values indicated in the figure. All of the compositions studied display structure in two frequency regimes; they show a relatively strong peak at ~370 cm^{-1}, with secondary features in some compositions, and a shoulder and weaker peak at ~150 cm^{-1}. The compound composition, $x=0.67$, and the S-rich alloys, $x=0.75$, 0.80, and 0.90, all have similar secondary features associated with the 370-cm^{-1} peak, a shoulder at ~410 cm^{-1} and a weaker feature at ~330 cm^{-1}. The maximum value of the reflectance at ~370 increases linearly with composition $(1-x)$ in the range from $x=0.90$ to $x=0.67$, and the reflectance at shorter wavelengths (~600 cm^{-1}) is approximately constant at a value of about 0.10. In the Ge-rich samples, $x=0.63$, 0.57, 0.55, there are marked changes in the character of the reflectance. For example, the secondary features associated with the 370-cm^{-1} peak are diminished in strength in the 0.63 sample and absent in the 0.57 and 0.55 samples. The reflectance peak at 370 cm^{-1} broadens and the short wavelength reflectance increases to approximately 0.15. It is interesting to note that unlike the higher-frequency features, there is very little change in the nature of the lower-frequency band (at ~150 cm^{-1}).

In a previously reported study of the ir reflectance of $Ge_{0.3}S_{0.7}$,[14] the spectrum was analyzed using damped harmonic oscillators. It was subse-

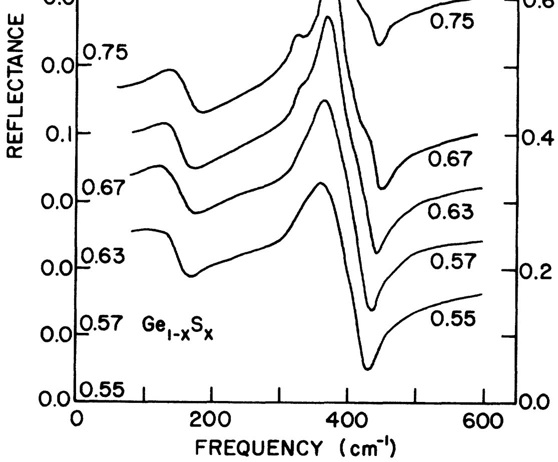

FIG. 1. Room-temperature ir reflectance spectra of bulk glasses in the alloy system $Ge_{1-x}S_x$. The spectra have been displaced for clarity with the zero values given along the left-hand edge of the figure.

quently reported that a better fit to a Kramers-Kronig (KK) derived ϵ_2 could be obtained using Gaussian-shaped oscillators.[23] The procedure we use to analyze the reflectance of the $Ge_{1-x}S_x$ alloys is the same as that used in Ref. 23. The objective of our analysis is to obtain an ϵ_2 spectrum which can then be used to study the compositional dependence of the dominant spectral features, in particular the oscillator which gives rise to the sharp reflectance peak near 370 cm^{-1}. For completeness we outline briefly the analytical procedure. The reflectance spectrum is first analyzed using damped harmonic oscillators; i.e., the experimental reflectance is fit with a reflectance that is synthesized from a complex dielectric constant, $\epsilon_c=\epsilon_1-i\epsilon_2$, constructed as a superposition of damped Lorentzian oscillators; i.e.,

$$\epsilon_c(\nu)=\epsilon_\infty+\sum_{j=1}^{N}\frac{S_j\nu_j^2}{\nu_j^2-\nu^2+i\Gamma_j\nu} . \qquad (1)$$

ν_j is the oscillator frequency of the jth mode (in cm^{-1}), S_j is the oscillator strength and contribution of the jth mode $\Delta\epsilon_0^j$ to the static dielectric constant ϵ_0, Γ_j is an empirical damping constant (in cm^{-1}), N is the number of oscillators, and ϵ_∞ is the optical-frequency dielectric constant. The experimental reflectance is then extended to both higher and lower cm^{-1} using a reflectance synthesized from the damped harmonic oscillators. The validity of this technique rests on the fact that the extension is made in frequency domains in which ϵ_2 is very small with respect to ϵ_1, so that the Lorentzian character of the oscillators is not the determinant factor. The analytically extended spectrum is then studied via a KK analysis. The harmonic oscillator fit to the reflectance spectrum of the compound composition is shown in Fig. 2. Four oscillators were employed in the fitting procedure; this number corresponds to the number of discernable features in the reflectance spectrum. The fit is good over most of the spectral range; however, the inability of Lorentzian oscillators to fit simultaneously the peak reflectance at ~370 cm^{-1} and the relative sharp minimum at ~450 cm^{-1} is an indication that the "real" ϵ_2 falls off faster than an idealized Lorentzian oscillator. This is indicated in Fig. 3 where we compare the ϵ_2 spectrum obtained from the oscillator analysis with an ϵ_2 spectrum obtained from the KK analysis of an analytically extended reflectance. The two ϵ_2 are in good agreement with respect to the width of the modes and their center frequencies; however the KK ϵ_2 falls off much faster with frequency particularly in the wings of the 370-cm^{-1} peak as we had anticipated. The emphasis in this paper will not be on the detailed aspects of the various fitting procedures, but is rather on the compositional dependence of features in the derived ϵ_2 spectrum. The example given above illustrates the superiority of KK procedure to the simple harmonic oscillator analysis.

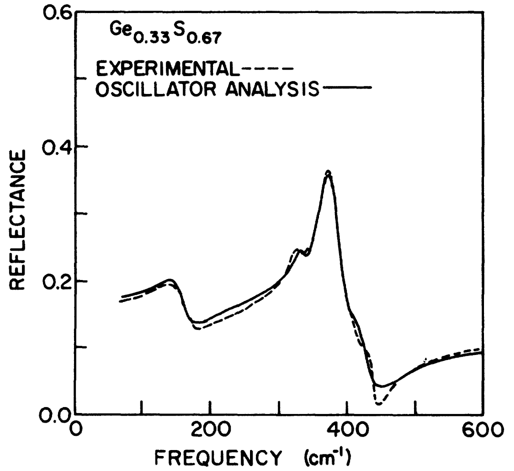

FIG. 2. Room-temperature ir reflectance spectrum of $Ge_{0.33}S_{0.67}$. The dashed curve is the experimental data, the solid curve is a four oscillator fit to the spectrum based on damped harmonic oscillators.

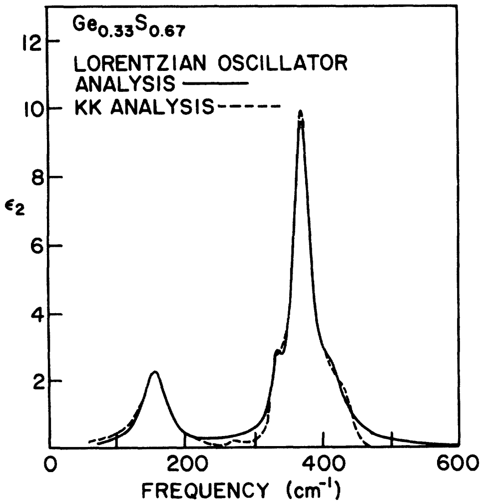

FIG. 3. Comparison of ϵ_2 spectra for $Ge_{0.33}S_{0.67}$ derived from the Lorentzian oscillator analysis (solid line) and from a KK analysis of an analytically extended reflectance (dashed line).

Figure 4 contains the KK-derived ϵ_2 spectra for the $Ge_{1-x}S_x$ system. As would have anticipated from our discussion of the reflectance spectra in Fig. 1, the ϵ_2 for the compound composition and the S-rich alloys all show similar features. The additional structures on the 370-cm^{-1} peak which are clearly evident for $x\geq 0.67$, diminish in the $x=0.63$ sample and are not observed in the $x=0.57$ and 0.55 samples. The magnitude of the maximum in ϵ_2 at ~370 cm^{-1} increases as x varies from 0.90 to 0.67 and then essentially remains constant; this

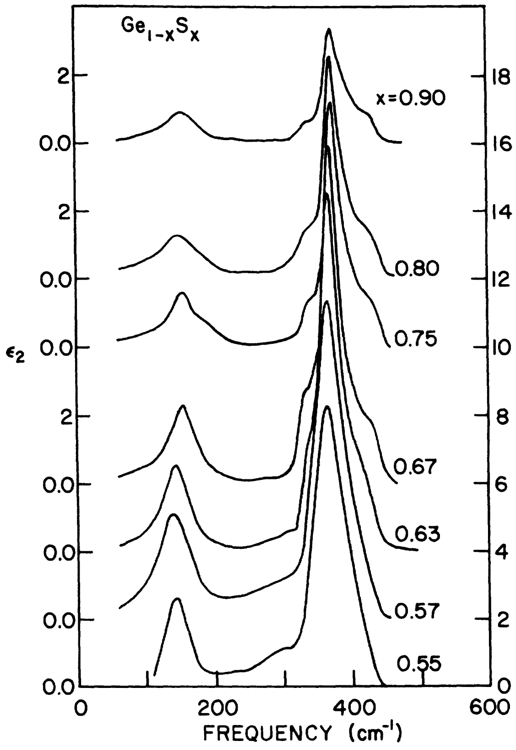

FIG. 4. Comparison of the KK-derived ϵ_2 spectra of glasses in the alloy system $Ge_{1-x}S_x$. The spectra of displaced for clarity with the zero values indicated at the left-hand edge of the figure.

behavior in ϵ_2 parallels that noted earlier for the maximum value of the reflectance. This trend will be examined in more detail in Sec. IV, where we consider the implications of chain crossing and random network structural models. We now go on to discuss the Raman spectra.

B. Raman spectra

In Figs. 5, 6, and 7 are displayed the Stokes-shifted Raman spectra of three of the alloys, the compound composition $x = 0.67$, a S-rich composition $x = 0.90$, and a Ge-rich composition $x = 0.63$, respectively. Each figure contains two spectra, one in the *HH* scattering configuration and the other in the *HV* configuration. The ratio of the scattering in these two configurations (*HV/HH*) defines a depolarization ratio[24] which contains the information about the symmetry characteristics of the nodes. All of our samples displayed some degree of optical inhomogeneity when viewed under polarizers. This means that the depolarization ratio can at best yield only qualitative information; i.e., we can assign relative depolarization ratios for the features in a given sample, but should not test the absolute ratios against any specific theories or models. Subject to this constraint, we find for example, that the 342-cm⁻¹ feature which is relatively strong in all of the glasses studied save the $x = 0.57$ sample is polarized, so that the mode giving rise to this feature is symmetric. In the S-rich glasses, three very sharp features occur at ~150, ~220, and ~475 cm⁻¹. These features all grow in strength relative to the 342-cm⁻¹ feature as the Ge content is reduced. The 150-cm⁻¹ mode is depolarized, whereas the other two modes are strongly polarized. Finally the 250-cm⁻¹ feature in the $x = 0.63$ sample (Fig. 7) is also strongly polarized. All other features show substantially weaker polarization effects.

We have reduced our experimental data for the *HH* spectra using the reduction scheme of Shuker-Gammon[25] as modified by Kobliska and Solin.[24] The reduced spectra are shown in Figs. 8 ($x = 0.90$, 0.80, 0.75, and 0.67) and 9 ($x = 0.67$, 0.63, and 0.57). The reduction scheme is based on the following equation:

$$\rho(\nu) = \nu(\nu_i - \nu)^{-4}(1 - e^{-h\nu/kT}) I_{HH}(\nu, T) \,. \qquad (2)$$

ν_i is the frequency of the incident (laser) photon (in cm⁻¹), ν is the frequency relative to the laser frequency, i.e., the phonon frequency (where $\nu = \nu_i - \nu_s$ and ν_s is the frequency of the scattered light), the temperature T enters through the Bose-Einstein occupation number for a phonon of energy

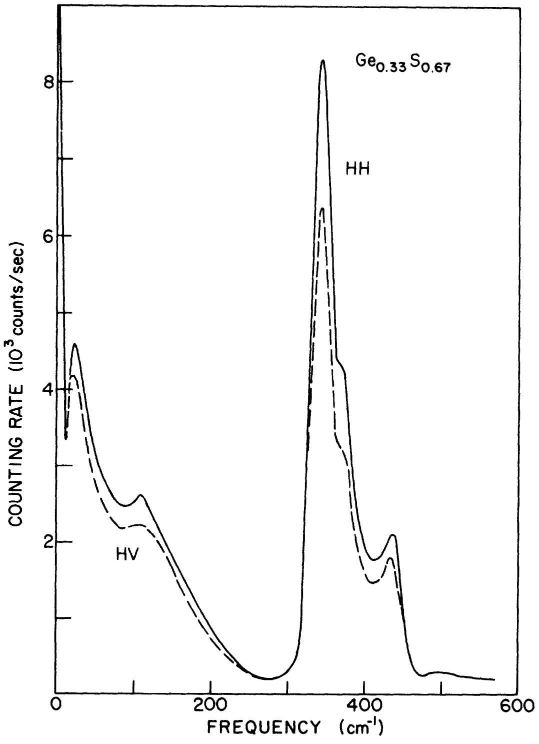

FIG. 5. Room-temperature *HH* and *HV* Raman spectra for $Ge_{0.33}S_{0.67}$.

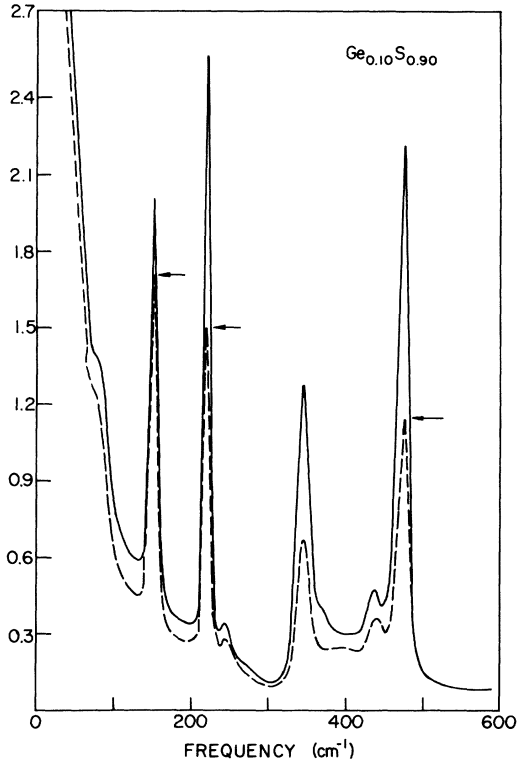

FIG. 6. Room-temperature *HH* and *HV* Raman spectra for $Ge_{0.10}S_{0.90}$. The arrows indicate the peak height of the scattering for the sharp modes in the *HV* geometry.

ν, $I_{HH}(\nu, T)$ is the scattered light intensity at a frequency shift ν (and in this equation is assumed to be corrected for any instrumental transfer characteristics), and $\rho(\nu)$ is a reduced spectrum, sometimes called an effective density of states.

The reduced spectra have been grouped into two figures in order to illustrate the similarities between certain features that occur in the S-rich glasses and the compound (Fig. 8) and also to illustrate the important changes that occur when the glass becomes Ge-rich (Fig. 9). The spectra in Fig. 8 have been adjusted so that the peak height of the sharp feature at ~342-cm^{-1} scales as $(1-x)$. This relative normalization is based on an assumption that the sharp Raman feature is associated with the same structural grouping, four S atoms in a tetrahedral arrangement about a Ge atom, as is the sharp ir feature (in ϵ_2) at ~367 cm^{-1}. The relative frequencies of these two modes, i.e., the ir feature being at a higher frequency than the Raman feature, are in quantitative agreement with a force constant calculation[14] based on a molecular model.[26] This normalization then provides a measure of the compositional dependence of the three sharp lines at ~150, ~220, and ~475 cm^{-1}. These lines are relatively weak in both $x = 0.75$ and 0.80 samples, but dominate in the $x = 0.90$ sample. A structural interpretation for their origin will be given in Sec. IV.

In Fig. 9 we compare the unnormalized Raman spectra of the two Ge-rich alloys with the compound. There is no evidence for line spectra as we have found in the S-rich glasses. The very sharp feature at 342 cm^{-1} diminishes in intensity in the 0.63 sample and is completely absent in the 0.57 sample. Furthermore, new broad features appear; in the 0.63 sample there is an asymmetric structure with its maximum scattering amplitude at ~250 cm^{-1}, and in the 0.57 sample there are broad features at ~220 and ~380 cm^{-1}. Recall that the $x = 0.57$ spectrum was obtained in a back-scattering geometry. In this sample the Raman scattering was superposed on a very strong Rayleigh background making it difficult to make quantitative comparisons that include this sample. This means that quantitative comparisons of Raman spectra for the Ge-rich regime include only the $x = 0.63$ and $x = 0.67$ samples.

In Sec. IV we analyze the trends in the spectra discussed in this section. As is evident from both the ir and Raman results, the problem can be partitioned into two regimes, the S-rich glasses $x > 0.67$ and the Ge-rich alloys $x < 0.67$, with the compound composition $x = 0.67$ playing a pivotal

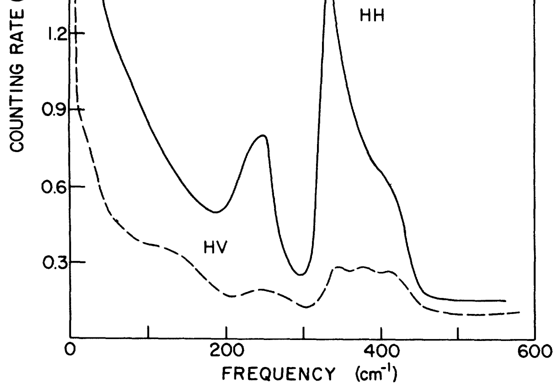

FIG. 7. Room-temperature *HH* and *HV* Raman spectra for $Ge_{0.37}S_{0.63}$.

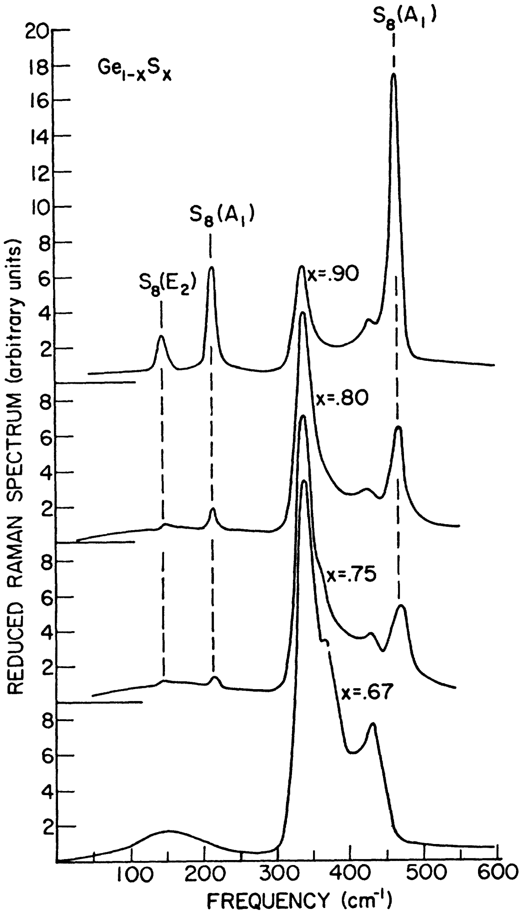

FIG. 8. Comparison of the reduced Raman spectra of the S-rich alloys ($x = 0.75$, 0.80, and 0.90) with the spectrum of the compound composition (0.67). The sharp line features in the three S-rich compositions are assigned to vibrational modes of S$_8$ molecules; the symmetries of these modes are also designated. The spectra in this figure have been normalized by assuming that the Raman scattering at the spectral peak (~ 342 cm^{-1}) is proportional to (1-x) where x is the sulfur concentration.

role. Our approach in Sec. IV will be to first discuss the compound composition and use the results of that analysis to understand the changes that occur in both the S-rich and Ge-rich compositions. The exercise we perform in Sec. IV represents the first attempt to use ir and Raman spectroscopy in a quantitative way to discriminate between competing structural models. The study of the Ge$_{1-x}$Se$_x$ system[13] used only Raman spectroscopy where variations in homogeneity (density fluctuations that give rise to index of refraction fluctuations) can give rise to problems in sample to sample comparisons. Our technique of using the ir results to quantify the comparison of Raman experiments should minimize these effects.

IV. STRUCTURAL INTERPRETATION

A. Compound composition, $x = 0.67$

It has been demonstrated[14] that the ir and Raman spectra of glassy Ge$_{0.30}$S$_{0.70}$, a composition close to the compound, could be understood in terms of a a structural model based on a chemically ordered phase. The element of local order was a tetrahedral arrangement of S atoms about a central Ge atom. The tetrahedra are connected into a network through the twofold coordinated S atoms. The model for this material is therefore similar to that proposed for the isoelectronic glass, fused SiO$_2$.[27]

Within the context of the tetrahedral model, the dominant and high-frequency features of the ir and Raman spectra at 367 and 343 cm^{-1} are associated, respectively, with the F_2 and A_1 modes of an XY_4 "molecule."[28] A model based on XY_4 also predicts two lower-frequency modes. There are features in both the ir and Raman spectra that occur in the same spectral range (100–150 cm^{-1}) as the predicted molecular modes (E_1: 114 cm^{-1}; F_2: 147 cm^{-1})[14]; however these structures are too broad to

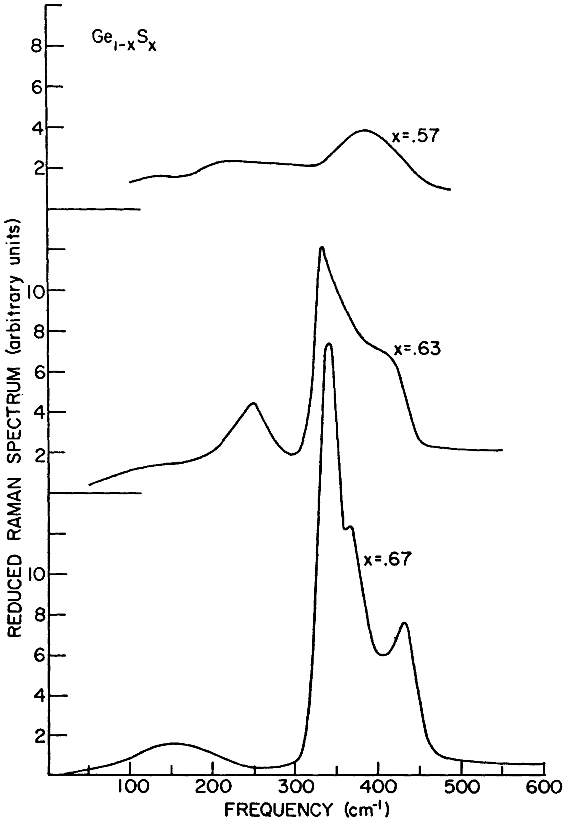

FIG. 9. Comparison of the reduced Raman spectra of the Ge-rich alloys ($x = 0.63$, 0.57) with the compound ($x = 0.67$). The data here are not normalized with respect to each other.

be of value in supporting a particular model. In the analysis that follows, we therefore use the sharp and spectroscopically isolated features in the ir and Raman spectra at 367 and 342 cm^{-1}, respectively, to characterize the structural element consisting of four S atoms in a tetrahedral configuration about a central Ge atom.

B. S-rich alloys, $x > 0.67$

We first consider the ir results. We have already pointed out the close similarity between the ir reflectance spectra of the S-rich glasses and the compound composition. That similarity is preserved in the ϵ_2 spectrum of Fig. 4 that were derived via the KK analysis. In all elemental amorphous solids studied to date, i.e., Ge,[29,30] si,[30] Se,[31] and As,[32] the ir-active modes are too weak to produce observable reflectance bands; structure is detectable only in ir transmittance measurements. It is therefore evident that the strong feature at ~370 cm^{-1} is due to a heteropolar bond, in this alloy system a Ge-S vibration. The issue is then whether that vibration is simply characteristic of a single Ge-S bond or a particular spatial arrangement of Ge and S atoms involving more than one S, e.g., a GeS_4 tetrahedron as suggested by the analysis of the $Ge_{0.30}S_{0.70}$ glass.[14] It is possible to distinguish between these two alternatives by considering the structural models that might be operative in this regime of alloy compositions.

We restrict our discussion to structural models based on nearest-neighbor covalent bonding, i.e., models which preserve a fourfold coordination at the Ge sites and a twofold coordination at the S sites. With this constraint imposed, there are two models to consider, the CCM[6,12] and the RCNM.[6,12] The CCM is based on an assumption of chemical ordering; i.e., it requires each Ge atom to be bonded to four S atoms and further, that the resultant GeS_4 tetrahedra are interconnected by chains of S atoms. The CCM was initially proposed for the $Ge_{1-x}Te_x$[6] and $Ge_{1-x}Se_x$[12] systems, in which the bonding tendency of the chalcogenide atom is to form chains rather than rings, i.e., the *trans*-conformation is preferred over the *cis*-conformation.[33] In the S system, the bonding tendency is toward ring formation so that a CCM must be generalized. The statistics of the bond types, i.e., whether they be Ge-S bonds or S-S bonds, is not changed by including the possibility of ring formation. The existence of a second species means that the solid must be viewed as a solution of rings in a network structure that includes GeS_4 tetrahedra. The existence of a second species in solution with a primary species is not to be confused with phase separation. Phase separation in a system implies inhomogeneity on an observable scale and is therefore differentiable from a homogeneous system, e.g., a solution of two different molecular species. In the $Ge_{1-x}Se_x$ system, one would also anticipate ring formation (Se_8 rings); however, the similar masses of Se and Ge, as well as a similarity between ringlike and chainlike frequencies[34] makes it difficult to isolate a second molecular species, particularly in the Raman studies.[13]

In a CCM based on four-two coordination, the numbers of Ge-S and S-S bonds/atom are given by[12]

$$\begin{array}{ll} \text{Ge-S:} & 4(1-x)\,, \\ \text{S-S:} & 3x-2\,, \end{array} \quad 1.00 \geq x \geq 0.67\,, \qquad (3)$$

where x is the S concentration. Using this notation, the total number of bonds/atom is $2-x$. In this model both bond types show a *linear* dependence on concentration; i.e., the number of Ge-S bonds increases as four times the Ge concentration $(1-x)$ as would be expected from the assumption of chemical ordering, and the number of S-S bonds is proportional to the S content, going to zero at the compound composition.

The alternative model is the RCNM in which all three possible bond types are involved. Assuming that all bond types are equally probable, i.e., that bond energies do not influence the statistics, it then follows that the number of bonds/atom are given by[12]

$$\begin{array}{ll} \text{Ge-Ge:} & 4(1-x)^2/(2-x), \\ \text{Ge-S:} & 4x(1-x)/(2-x), \\ \text{S-S:} & x^2/(2-x). \end{array} \qquad (4)$$

In this model the increase in the number of Ge-S bonds with $1-x$ is sublinear and the decrease in the number of S-S bonds with x is superlinear.

In Fig. 10 we plot the concentration of Ge-S bonds/atom as a function of S content for the two models, CCM and RCNM. Also included in the figure are the maximum values of ϵ_2 at the 367-cm^{-1} spectral peak. The experimental ϵ_2 have all been divided by a single number, chosen so that a least-squares fit of the normalized experimental ϵ_2' to a dependence $\epsilon_2' = a(1-x)$ has a value of 1.33 at $x = 0.67$. It is evident that these experimental results cannot be reconciled with the RCNM but do fit the CCM. Since the CCM is based on chemical ordering, the linear dependence in ϵ_2, illustrated in Fig. 10, lends support to the conclusions of the study on the $Ge_{0.30}S_{0.70}$ glass, namely, that the 367-cm^{-1} feature in the ir reflectance is associated with a tetrahedral grouping of S atoms about a central Ge atom.

The linearity of ϵ_2, and the assignment of the 367-cm^{-1} mode to the GeS_4 tetrahedron support the normalization of the reduced Raman data for $x \geqslant 0.67$. The spectra shown in Fig. 8 have been normalized according to a linear dependence

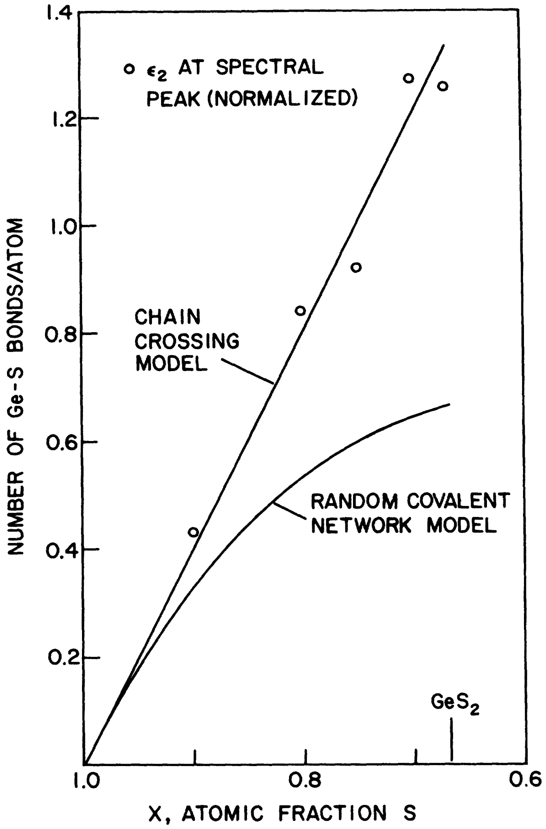

FIG. 10. Number of Ge–S bonds/atom as a function of x, the S concentration for the CCM and the RCNM. The experimental values of ϵ_2 have all been divided by a single number so that a least squares fit of the experimental ϵ_2 to the $4(1-x)$ dependence of the CCM gives a value of 1.33 at $x = 0.67$. The ϵ_2 for the $x = 0.70$ sample is obtained using the data from Ref. 14.

$(1-x)$ in the peak value for the 342-cm^{-1} feature. In the context of our analysis, this mode is also is also associated with the GeS_4 tetrahedron and should therefore have the same compositional dependence as the ir mode of the same cluster. The primary purpose of the normalization of Raman spectra is to understand the way the "excess" S atoms are coordinated into the glasses in the S-rich regime; e.g., whether they are all contained in chainlike elements between the Ge sites, or whether there is a monomer or ring species also present.

Before attempting to identify a specific structural configuaration by the frequencies and symmetry character of the modes, we can rule out one of the structural possibilities by scaling arguments. If we take the CCM literally, and simply associate the three sharp line features in the Raman scattering with S-S bonds, then we would expect the scattering in these lines to scale as $3x-2$. The intensities are clearly nonlinear with composition and rule out this explanation. However, by first identifying the structural origin of these modes, it is then possible to explain their compositional dependence. The sharp line features occur at almost exactly the frequencies of the dominant Raman modes of an S_8 molecule as they are determined from studies of crystalline orthorhombic S,[35] or liquid S.[36] Furthermore, the depolarization characteristics are also consistent with this assignment. As we noted earlier, ir reflectance studies are useful in detecting heteropolar bonds, but cannot in general identify the presence of homopolar bonds. We have therefore compared the ir transmittance of two alloys compositions, the compound composition $x = 0.67$ and a S-rich composition, $x = 0.90$. The compound composition shows strong absorption in the neighborhood of the reflectivity peaks, from 460 to 300 cm^{-1} and below 200 cm^{-1}, and is relatively transparent in other regions. The S-rich composition has additional absorption lines at ~475 and ~240 cm^{-1}. These correlate with two of the three dominant absorption bands of S_8 molecules[37]; a third band expected at ~185 cm^{-1} is obscured by the strong and broad absorption associated with the 155-cm^{-1} reflectance band.

There are several possible ways in which the S_8 molecule population could vary with the S content. If either steric hindrance, or relative bond strength mechanisms were operative, either or both of these could limit the number of S atoms incorporated between Ge atoms. For example, if only one S atom were allowed between each Ge atom, and the rest of the S went into S_8 rings we would anticipate a linear dependence of S_8 population on x. This is clearly not the case. However, the occurrence of S_8 modes in the $x = 0.75$ sample indicates that there are probably a small number of local configurations where there is indeed only one S between the Ge atoms. On the other hand, if two S atoms were allowed, then we would expect an abrupt rise in the S_8 ring population for $x > 0.80$. This is the case, as is illustrated in Fig. 11. Here we have plotted the expected S_8 populations for two models; model I in which only one atom can be incorporated between neighboring Ge sites, and model II in which two S atoms are included. The experimental points represent the average scattering intensity in the S_8 modes as determined from the normalized Raman scattering. The intensities for the $x = 0.75$ and $x = 0.80$ samples are fit to model I and indicate that approximately 0.40 of the Ge sites are separated by only one S atom. The remaining experimental point then falls on a composite curve which assumes that ~0.60 of the Ge sites are separated by two S atoms. The results reported here are consistent with dissolution studies[21] which indicate a similar rise in the S_8 concentration for $x > 0.80$. The incorporation

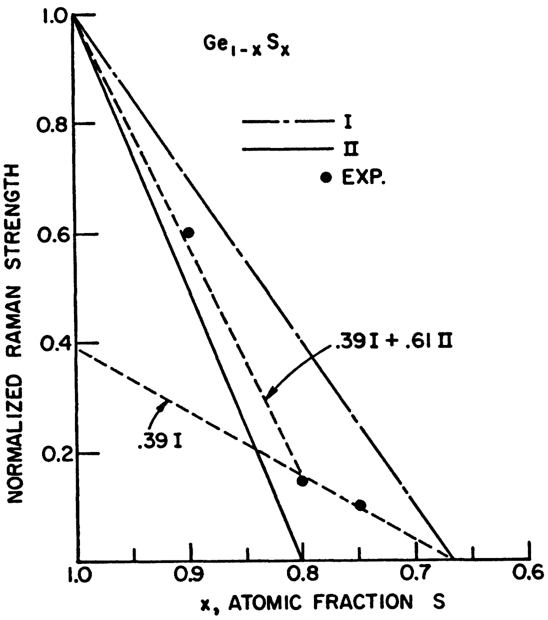

FIG. 11. Plot of normalized Raman scattering in the three S_8 modes of the S-rich glasses as a function of x, the atomic fraction of S. The data are compared with two model calculations: Model I (— — —) in which only one S atom is allowed between Ge sites, and model II (———) in which two S atoms are included between the Ge sites. The experimental points have been normalized to fit model I for $x = 0.75$ and $x = 0.80$. The scattering at $x = 0.90$ then falls on a line (0.39 I + 0.61 II) which assumes that there are at least two kinds of atomic configurations corresponding to models I and II.

of no more than two S atoms between the Ge atoms is related to the bonding tendencies of S. Incorporation of three S atoms in a ring conformation would interfere with the Ge-S network. On the other hand, a tendency toward the chain conformation as in $Ge_{1-x}Se_x$ could accommodate a larger number of chalcogenide atoms.

C. Ge-rich alloys, $x < 0.67$

Unfortunately, the kinetics associated with crystallization do not permit glass formation deep into the Ge-rich regime. This means that any conclusions we draw from our study of the Ge-rich regime concerning local environments are necessarily more restrictive than those conclusions we were able to make concerning local order in the S-rich regime. Any extrapolation of our results through the entire Ge-rich to *a*-Ge is therefore speculative. For example, our experiments do not rule out different local coordinations in the vicinity of a second compound composition corresponding to GeS ($x = 0.5$).

A comparison of the KK derived ϵ_2 for the Ge-rich alloys with the ϵ_2 of the compound (see Fig. 4) demonstrates that significant changes in the ϵ_2 spectrum occur for relatively small changes in alloy composition. The important changes in the ϵ_2 spectra reflect the changes already noted in the reflectance spectra and include the loss of the high and low frequency shoulders to the 370-cm^{-1} line, and an increase by about a factor of 2 in the width of this feature. A similar situation exists for a comparison of the reduced Raman spectra (see Fig. 9). There are two structural models which can be operative in the Ge-rich alloy regime that preserve the four-two coordination (at Ge and S sites, respectively) that is required by simple covalent bonding in which the $8 - N$ rule is satisfied. Only one of these models is able to account for the changes in the character of the spectra that are noted above, the same model is also the only one which is capable of providing continuity across the compound composition.

The first model is the RCNM discussed in Sec. IV B. This model is based simply on statistics and coordination, with no preference toward chemical ordering. The second model is based on an assumption of chemical ordering and has been used by Philipp[17] in interpreting the optical properties of SiO_x films. In this model one assumes that there are no S-S bonds, and therefore can characterize the local order through five types of tetrahedra. Explicitly, one considers all of the tetrahedral types to have a central Ge atom; the four other atoms are then attached to the central Ge atom according to the statistics of the composition. If $\bar{x}$ is the S fraction normalized to the compound composition, i.e., $\bar{x} = \frac{1}{2}[x/(1-x)]$, and $\bar{x} + \bar{y} = 1$, then the distribution of tetrahedra is given by

$$\begin{aligned} &GeS_4: && \bar{x}^4, \\ &GeS_3Ge: && 4\bar{x}^3\bar{y}, \\ &GeS_2Ge_2: && 6\bar{x}^2\bar{y}^2, \\ &GeSGe_3: && 4\bar{x}\bar{y}^3, \\ &GeGe_4: && \bar{y}^4, \end{aligned} \tag{5}$$

and displayed in Fig. 12.

We have already argued that the sharp peak in ϵ_2 at 367 cm^{-1} and a similar feature in the reduced Raman spectrum at 342 cm^{-1} are associated with a tetrahedral arrangement of four S atoms about a Ge atom. The dramatic changes in these two sharp features upon alloying into the Ge-rich region are well correlated with the rapid decrease in the GeS_4 population. Note that in the Philipp's model, at $x = 0.63$ only about half of the Ge atoms have four S neighbors, and at $x = 0.57$, less than 0.20 of the Ge have four S neighbors. The existence of an observable peak at 342 cm^{-1} in the $x = 0.67$ and $x = 0.63$ Raman spectra is in agreement with the Philipp's model. However, the absence

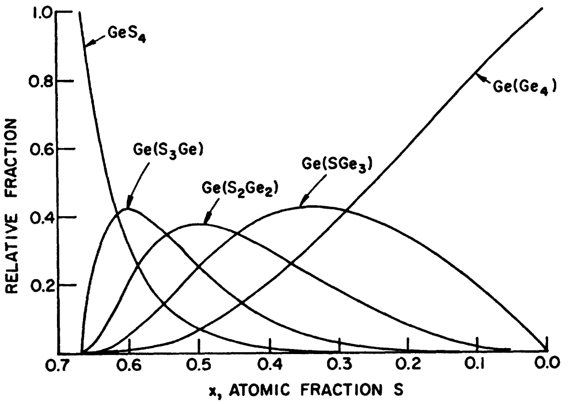

FIG. 12. Relative fraction vs composition x, of the five types of tetrahedra allowed by the Philipp's model (Ref. 17). At $x = 0.67$ there only GeS$_4$ tetrahedra and at $x = 0.00$ only Ge (Ge$_4$) tetrahedra. At intermediate compositions, there are five types of tetrahedra $GeS_{4-n}Ge_n$ ($n = 0$, 1, 2, 3, 4).

of a peak at 342 cm^{-1} in the $x = 0.57$ Raman spectrum may be associated with a more rapid depletion of the GeS$_4$ population than is predicted by the Philipp's model, or alternatively this feature may be shifted to higher frequencies and broadened due to solid state interactions which become increasingly important as the number of four-coordinated Ge-sites is increased. However, ir spectra indicate a peak at ~370 cm^{-1} in both the $x = 0.57$ and $x = 0.55$ samples; we take the ir results to imply some portion of GeS$_4$ local configurations. We also demonstrate that additional features in the spectra, e.g., the Raman mode at 250 cm^{-1} in the $x = 0.63$, are consistent with existence of local order elements that contain fewer than four S atoms. These dramatic changes in the character of the spectra for small changes in x cannot be reconciled with RCNM. In that model the number of S-S, GeGe, and Ge-S bonds all show small and smoothly varying changes with no abrupt discontinuities in slope at the compound composition.

It has already been demonstrated that the high frequency features of the $Ge_{0.30}S_{0.70}$ spectra were in accord with a molecular model based on a GeS$_4$ tetrahedron.[14] In Ref. 14, molecular frequencies for GeS$_4$ were estimated by scaling the frequencies of a GeCl$_4$ molecule. It was further demonstrated that the scale factor was consistent with the difference in mass between S and Cl and with the differences in ionicity between Ge and S atoms, and Ge and Cl atoms. There have also been studies made on other Ge-tetrahalide molecules, GeBr$_4$ (Ref. 38) and compounds containing both Cl and Br, $GeCl_{4-n}$ (Ref. 38) ($n = 0, 1, 2, 3, 4$). These other molecules can be expected to serve respectively as models for GeSe$_2$ composition, and alloys along the pseudobinary join from GeS$_2$ to GeSe$_2$, i.e., $GeS_{2-x}Se_x$. In these materials the tetrahedra are "isolated" in the spirit of the molecular model[26] by the twofold coordinated chalcogenide atoms. For qualitative purposes, we extend the molecular model, and estimate the frequencies of tetrahedra containing less than four chalcogenide atoms by comparisons with the mixed tetrahalide molecules. This estimate neglects line-broadening effects which are expected to become increasingly important as the Ge content increases. We find that GeS$_3$Ge and GeS$_2$Ge$_2$ are expected to have symmetric Raman modes in the vicinity of 230–24 cm^{-1} and suggest this can be used to assign the 250-cm^{-1} feature in the $x = 0.63$ sample to tetrahedra with fewer than four S atoms. We believe that the 215-cm^{-1} feature in the $x = 0.57$ sample has a similar structural association, however, this is more speculative.

One attractive argument for invoking the Philipp's model for the Ge-rich regime is that it blends continuously into the CCM at the compound composition, GeS$_2$. Both models give a chemically ordered phase at $x = 0.67$ with only Ge-S bonds. The Philipp's model also extrapolates to the correct local order for a-Ge. However, it is entirely possible, as already noted, that the alloys with $x < 0.55$ may have additional elements of local bonding. Studies of this system should be extended to include amorphous films produced by techniques such as evaporation, sputtering, or chemical vapor deposition, to probe further into the Ge-rich regime.

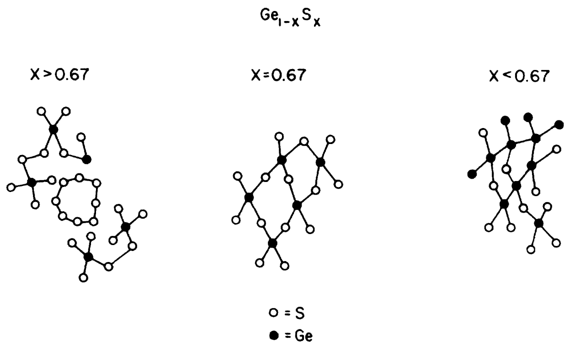

FIG. 13. Schematic representation of the local order in the system $Ge_{1-x}S_x$. At the compound composition, $x = 0.67$, there is a chemically ordered network of four-coordinated Ge and two-coordinated S. In the S-rich regime, $x > 0.67$ there exists a solid solution of S$_8$ ring molecules in a matrix of GeS$_4$ tetrahedra which are interconnected by either one or two S atoms. In the Ge-rich regime, $x < 0.67$, there is a network structure containing Ge–Ge bonds and Ge–S bonds, but no S–S bonds. This network can be described in terms of five types of tetrahedra centered on Ge atoms, $GeS_{4-n}Ge_n$ ($n = 0$, 1, 2, 3, 4).

V. DISCUSSION

We have used ir and Raman spectroscopy to distinguish between competing structural models for the alloy system, $Ge_{1-x}S_x$. For S-rich alloys a CCM applies; this model allows only Ge-S and S-S bonds. In the S-rich region the system is essentially a solid solution consisting of a network of very short S chains cross linked by four-coordinated Ge atoms, and a monomer component of S_8 ring molecules. The number of S atoms between the Ge-sites is small, of the order of 1 to 2; this is evidenced by a very rapid increase in the S_8 population for S concentrations in excess of $x = 0.80$. This tendency toward ring formation is confirmed by other studies; for example the dissolution studies in Ref. 21. At the compound composition the glass is chemically ordered and has a local configuration similar to fused SiO_2.[27] For the Ge-rich alloy regime, we have not been able to describe the system in the same detail as for the S-rich regime. The limitation in this study is the availability of bulk glasses. The ir and Raman spectra of the glasses formed in this regime, $x = 0.63$, $x = 0.57$, and $x = 0.55$, are consistent with the extension of Philipp's model for the SiO_x system to the Ge-rich regime of the Ge-S system.

Figure 13 is a schematic representation of the bonding tendencies in this alloy system. For the S-rich regime we indicate the two species identified through the ir and Raman studies, a network structure based on a local GeS_4 configuration, but linked together through a limited number of S atoms and a molecular species S_8. For the compound, we indicate a chemically ordered phase based on GeS_4 tetrahedra. For Ge-rich alloys, we show a network structure that exemplifies the application of the Philipp's model to the Ge-S system.

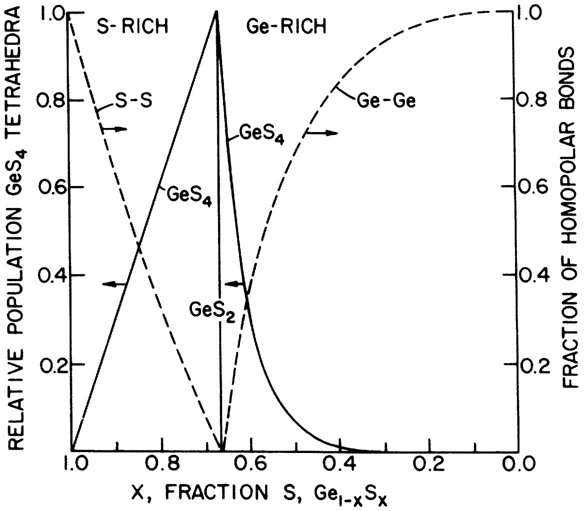

FIG. 14. Summary of some of the important elements of local order in the $Ge_{1-x}S_x$ alloy system. The relative population of GeS_4 tetrahedra is described by the CCM in the S-rich regime and by the Philipp's model (Ref. 17) in the Ge-rich regime. At the compound composition, GeS_2, there are only Ge-S bonds and the structural element is GeS_4 tetrahedron. In the S-rich regime the fraction of S-S bonds decreases going to zero at $x = 0.67$. In the Ge-rich regime, the fraction of Ge-Ge bonds increases from 0.0 at $x = 0.67$ to 1.0 at $x = 1.0$.

Figure 14 illustrates the compositional dependence of the important elements of local order in this system, the GeS_4 tetrahedra, and the relative fraction of S-S and Ge-Ge bonds. The curves in the figure are developed from the CCM for the S-rich regime and the Philipp's model for the Ge-rich regime. We have clearly demonstrated the applicability of the CCM to the S-rich regime, but have only been able to argue for the applicability of the Philipp's model in a restricted region of the Ge-rich regime ($0.67 > x > 0.55$). It would be of considerable interest to pursue alloy compositions with larger Ge concentrations than can be quenched in bulk form. These studies could determine the applicability of an extrapolation of the Philipp's model through the Ge-rich regime to pure *a*-Ge.

ACKNOWLEDGMENTS

The authors have benefited from discussions with T. M. Hayes, S. S. Oren, P. N. Sen, and G. B. Fisher. We also acknowledge the assistance of W. Mosby in the Raman measurements.

---

[1] A. Bienenstock, F. Betts and S. R. Ovshinsky, J. Non-Cryst. Solids 2, 347 (1970).

[2] D. B. Dove, M. B. Heritage, K. L. Chopra, and S. K. Bahl, Appl. Phys. Lett. 16, 138 (1970).

[3] R. W. G. Wyckoff, *Crystal Structures* (Wiley, New York, 1963), Vol. 1.

[4] A. Bienenstock, J. Non-Cryst. Solids 11, 447 (1973).

[5] N. F. Mott, Adv. Phys. 16, 49 (1967).

[6] F. Betts, A. Bienenstock, and S. R. Ovshinsky, J. Non-Cryst. Solids 4, 554 (1970).

[7] F. Betts, A. Bienenstock, D. T. Keating, J. P. de Neutville, J. Non-Cryst. Solids 7, 417 (1972).

[8] G. B. Fisher, J. Tauc, and Y. Verhelle, in *Proceedings of The Fifth International Conference on Liquid and Amorphous Semiconductors*, edited by J. Stuke and W. Brenig (Taylor and Francis, London, 1974), p. 1259.

[9] G. B. Fisher and W. E. Spicer, J. Non-Cryst. Solids 8-10, 973 (1972).

[10] G. B. Fisher, I. Lindau, B. A. Orlowski, W. E. Spicer, Y. Verhelle, and H. E. Weaver, in Ref. 8, p. 621.

[11] N. J. Shevchik, J. Tejeda, D. W. Langer, and M. Cardona, Phys. Rev. Lett. 30, 659 (1973); Phys. Sta-

tus Solidi 57, 245 (1973).

[12] F. W. Fawcett, C. N. J. Wagner, and G. S. Cargill III, J. Non-Cryst. Solids 8-10, 369 (1972).

[13] P. Tronc, M. Bensoussan, and A. Brenac, Phys. Rev. B 8, 5947 (1973).

[14] G. Lucovsky, J. P. deNeufville, and F. L. Galeener, Phys. Rev. B 9, 1591 (1974).

[15] S. C. Rowland, S. Narasimhan, and A. Bienenstock, J. Appl. Phys. 43, 2741 (1972).

[16] L. Cervinka and A. Hruby, in Ref. 8, p. 431.

[17] H. R. Philipp, J. Non-Cryst. Solids 8-10, 627 (1972).

[18] G. Lucovsky, in Ref. 8, p. 1099.

[19] M. Hansen, *Constitution of Binary Alloys* (McGraw-Hill, New York, 1958).

[20] Y. Kawamoto and S. Tsuchihashi, J. Am. Ceram. Soc. 52, 627 (1969).

[21] Y. Kawamoto and S. Tsuchihashi, J. Am. Ceram. Soc. 54, 131 (1971).

[22] D. Clark and W. Varney, *Physical Metallurgy* (Van Nostrand, Princeton, N. J., 1953).

[23] F. L. Galeener, G. Lucovsky, and M. Rodoni, Bull. Am. Phys. Soc. 19, 315 (1974).

[24] R. J. Kobliska and S. A. Solin, Phys. Rev. B 8, 756 (1973).

[25] R. Shuker and R. W. Gammon, Phys. Rev. Lett. 21, 222 (1970).

[26] G. Lucovsky and R. M. Martin, J. Non-Cryst. Solids 8-10, 185 (1972).

[27] R. J. Bell, N. F. Bird, and P. Dean, J. Phys. C 1, 299 (1968).

[28] G. Herzberg, *Infrared and Raman Spectra of Polyatomic Molecules* (Van-Nostrand-Rheinhold, New York, 1945).

[29] R. W. Stimets, J. Waldman, J. Lin, F. Chang, R. J. Temkin, G. A. N. Connell, and H. R. Fetterman, in Ref. 8, p. 1239.

[30] M. H. Brodsky and A. Lurio, Phys. Rev. B 9, 1646 (1974).

[31] G. Lucovsky, in *Physics of Selenium and Tellurium*, edited by W. C. Cooper (Pergamon, Oxford, 1969), p. 255.

[32] J. C. Knights, G. Lucovsky, and F. L. Galeener, Bull. Am. Phys. Soc. 19, 213 (1974); and G. Lucovsky and J. C. Knights, Phys. Rev. B 10, 4324 (1974).

[33] H. Krebs, *Fundamentals of Inorganic Crystal Chemistry* (McGraw-Hill, London, 1968).

[34] G. Lucovsky and R. M. Martin (unpublished).

[35] A. T. Ward, J. Phys. Chem. 72, 744 (1968).

[36] A. T. Ward, J. Phys. Chem. 72, 4133 (1968).

[37] D. W. Scott, J. P. McCullough, and F. H. Kruse, J. Molec. Spectrosc. 13, 313 (1964).

[38] K. Nakamoto, *Infrared Spectra of Inorganic and Coordination Compounds* (Wiley, New York, 1963).